PHYSICAL REVIEW D **89,** 014509 (2014)

On the definition and interpretation of a static quark-antiquark potential in the color-adjoint channel

Owe Philipsen and Marc Wagner

Goethe-Universität Frankfurt am Main, Institut für Theoretische Physik, Max-von-Laue-Straße 1, D-60438 Frankfurt am Main, Germany

(Received 18 October 2013; published 22 January 2014)

We study possibilities to define a static quark-antiquark pair in a color-adjoint orientation based on Wilson loops with generator insertions, using both lattice QCD and leading-order perturbation theory in various gauges. Nonperturbatively, the only way to obtain nonzero results while maintaining positivity of the Hamiltonian is by using either temporal gauge or Coulomb gauge with some additional constraint on the temporal links removing the residual gauge symmetry. In this case the correlator is equivalent to a gauge invariant correlation function of a static quark-antiquark pair and a static adjoint quark; the resulting three-point potential is attractive. Saturating open color indices with color magnetic fields instead also leads to a gauge invariant correlator. However, this object is found to couple to the singlet sector only and results in a hybrid potential. None of the considered lattice observables reproduces the repulsive adjoint potential predicted by perturbation theory in Lorenz or Coulomb gauges.

DOI: 10.1103/PhysRevD.89.014509 PACS numbers: 11.15.Ha

I. INTRODUCTION

Heavy quarkonium systems are most conveniently treated by means of effective theory methods like nonrelativistic QCD (NRQCD) [1,2] or potential nonrelativistic QCD (pNRQCD) [3,4]. In such frameworks the heavy quark mass gets integrated out, which to leading order results in a static quark propagator, i.e. a temporal Wilson line. The correlation function of a quark-antiquark pair at separation r then factorizes into a free propagator and the Wilson loop, whose exponential falloff at large correlation time defines the static quark-antiquark potential.

Ever since the early treatments [5–7] there has been interest in the color-adjoint (or octet for $N = 3$) channel, where the quark-antiquark pair is in the adjoint of its product representation of $SU(N)$, $N \otimes \bar{N} = 1 \oplus (N^2 - 1)$, and hence the corresponding mesonic states carry color charge. While these are clearly ruled out as asymptotic states of the particle spectrum, they naturally appear as intermediate states in the framework of NRQCD, pNRQCD or in the presence of a medium like the quark gluon plasma [8,9]. A perturbative definition after gauge fixing to Lorenz or Coulomb gauge appears to be straightforward and to leading order one finds [5]

$$(N^2 - 1)V^{T^a}(r) = -V^1(r) + \mathcal{O}(g^4) \qquad (1)$$

(V^1 denotes the singlet, V^{T^a} the color-adjoint static potential), where higher-order corrections are also known (cf. e.g. [4,10–12]). However, the question of a nonperturbative generalization is still open. Attempts to decompose Polyakov loop correlators defined at finite temperature into singlet and adjoint channels [6,7] were shown to fail nonperturbatively, since the exponential decay of both channels is governed by the color-singlet potential and the difference between them due to gauge-dependent matrix elements [13,14].

In this paper we discuss the static quark-antiquark potential in the color-adjoint channel at zero temperature based on the Wilson loop with generator insertions, as defined in Sec. II. This correlator is gauge dependent, and its nonperturbative evaluation requires gauge fixing. Lorenz gauges, which are commonly used in perturbation theory, are known to violate positivity and hence preclude the definition of a transfer matrix as well as a purely exponential decay of the correlator. Therefore, we mainly work with a temporal gauge which preserves those properties. We study the resulting correlation functions by spectral analysis in terms of the transfer matrix (Sec. III) and compute some of them numerically for $SU(2)$ (Sec. V). We also discuss the use of Coulomb gauge, which allows for a well-defined transfer matrix too [15]. However, nonperturbatively it requires a completion which can be implemented by a reduced form of temporal gauge. On the other hand, saturating the open adjoint indices with color-magnetic fields, as suggested in the literature [4], produces a gauge invariant observable but spectral analysis shows it to project on the color-singlet channel only. In Sec. IV we compare with leading-order perturbative calculations in the continuum using various gauges.

Our main results are

(1) In temporal gauge, the Wilson loop with generator insertions is equivalent to a gauge invariant quantity, where the generators are connected by an adjoint Schwinger line.

(2) Nonperturbatively, both in temporal as well as in "completed Coulomb gauge," the color-adjoint static potential corresponds to a system of three static quarks, two fundamental and one adjoint quark, which form a color-singlet state; this is in contrast to perturbatively calculated color-adjoint static potentials in Lorenz or Coulomb gauge, where no adjoint quark is present.

(3) The nonperturbative color-adjoint static potential is attractive (with even stronger binding than in the usual singlet channel), while the perturbative color-adjoint static potential in Lorenz or Coulomb gauge is repulsive [cf. Eq. (1)].

(4) The repulsive color-adjoint potential obtained in perturbation theory cannot be reproduced by any lattice observable considered here, not even at short distance.

Parts of this work have been presented at a conference [16].

II. STATIC POTENTIALS BASED ON WILSON LOOPS

The definition and calculation of the potentials between a static quark and antiquark at distance $|\mathbf{x}-\mathbf{y}|$, each in the fundamental representation, is usually based on the trial states

$$|\Phi^\Sigma(\mathbf{x},\mathbf{x}_0,\mathbf{y})\rangle \equiv \bar{Q}(\mathbf{x})U^\Sigma(\mathbf{x},\mathbf{y})Q(\mathbf{y})|0\rangle. \tag{2}$$

Here Q and $\bar{Q}$ are static quark and antiquark operators that are treated as spinless (one component) color charges, since the spin decouples from the Hamiltonian in the static limit,

$$U^\Sigma(\mathbf{x},\mathbf{y}) \equiv U(\mathbf{x},\mathbf{x}_0)\Sigma U(\mathbf{x}_0,\mathbf{y}), \tag{3}$$

Σ is an $N\times N$ matrix in the fundamental color representation and $U(\mathbf{x},\mathbf{y})$ is a gluonic string represented by a straight spatial Wilson line connecting $\mathbf{x}$ and $\mathbf{y}$. Hence, $|\Phi^\Sigma(\mathbf{x},\mathbf{x}_0,\mathbf{y})\rangle$ is a static meson with color transformation properties determined by Σ. For $\Sigma = 1$ it is a color singlet, whereas for $\Sigma = T^a$, the generators of the $SU(N)$ gauge group, it carries color charge and transforms in the adjoint representation of $SU(N)$ at $\mathbf{x}_0$.

If there exists a positive Hamiltonian, the correlation functions of these states in Euclidean time decay exponentially with eigenvalues of the Hamiltonian. In the static limit, i.e. for heavy quarks of mass $M\to\infty$, the correlators factorize in products of free static propagators and Wilson loops,

$$\langle\Phi^\Sigma(t_2;\mathbf{x},\mathbf{x}_0,\mathbf{y})|\Phi^\Sigma(t_1;\mathbf{x},\mathbf{x}_0,\mathbf{y})\rangle = e^{-2M\Delta t}N\langle W_\Sigma(r,\Delta t)\rangle,$$
$$W_\Sigma(r,\Delta t) \equiv \frac{1}{N}\mathrm{Tr}(\Sigma U_R \Sigma^\dagger U_L) \tag{4}$$

with $r\equiv|\mathbf{x}-\mathbf{y}|$ and $\Delta t \equiv t_2 - t_1 > 0$ (cf. Fig. 1). The exponential decay of the Wilson loop defines the corresponding static potentials,

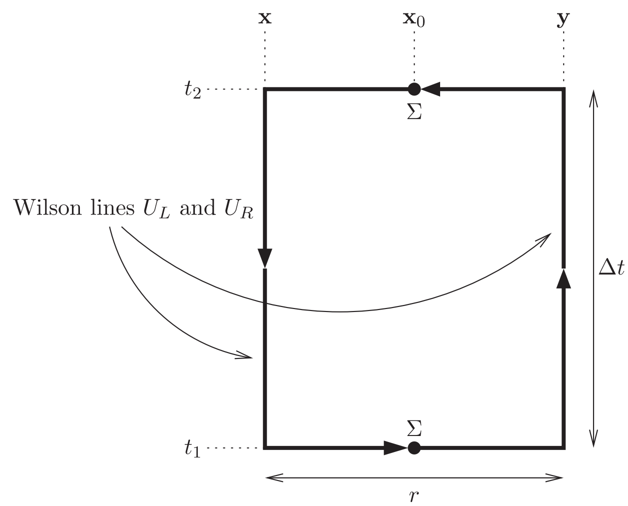

FIG. 1. The Wilson loop W_Σ.

$$\begin{aligned}\langle W_\Sigma(r,\Delta t)\rangle &= \sum_{n=0}^\infty c_n \exp(-V_n^\Sigma(r)\Delta t)\\ &= c_0\exp(-V_0^\Sigma(r)\Delta t)\\ &\quad\times(1+\mathcal{O}(\exp(-(V_1^\Sigma(r)-V_0^\Sigma(r))\Delta t)))\\ &\overset{\Delta t\to\infty}{\propto} \exp(-V^\Sigma(r)\Delta t).\end{aligned} \tag{5}$$

From the behavior at asymptotically large time separation the ground state potentials $V^\Sigma(r)\equiv V_0^\Sigma(r)$, $\Sigma\in\{1,T^a\}$ can be extracted. This is often used to define the ground state potentials directly through the corresponding Wilson loops,

$$V^\Sigma(r) = -\lim_{\Delta t\to\infty}\frac{d}{d\Delta t}\ln(\langle W_\Sigma(r,\Delta t)\rangle) = -\lim_{\Delta t\to\infty}\frac{\langle\dot{W}_\Sigma(r,\Delta t)\rangle}{\langle W_\Sigma(r,\Delta t)\rangle}. \tag{6}$$

The properties and interpretation of the potentials depend on Σ and, in case of $\Sigma = T^a$, on the choice of the gauge fixing condition. Without gauge fixing, a nonperturbative evaluation of the correlator gives

$$\langle W_{T^a}(r,\Delta t)\rangle = 0 \ (\text{no sum over } a). \tag{7}$$

For $N = 2, 3$ the corresponding static potential is usually called triplet/octet static potential and $T^a = \sigma^a/2$, $\lambda^a/2$.

It has been proposed to alternatively base the definition of the color-adjoint static potential on a gauge invariant correlator using e.g. $\Sigma = T^a\mathbf{B}^a(\mathbf{x}_0)$, where the adjoint transformation behavior of the color-magnetic field cancels that of the strings at $\mathbf{x}_0$. This yields a nonvanishing correlation function even without gauge fixing, from which one can extract so-called hybrid potentials (cf. e.g. [17–19]), which to leading and higher orders in a multipole expansion in small $|\mathbf{x}-\mathbf{y}|$ receive contributions from the adjoint channel [4]. However, we shall show in Sec. IIIA4 that nonperturbatively the eigenstates contributing to the exponential decay are in the color-singlet sector (as are hybrid potentials in general) and hence this correlator cannot be used for a nonperturbative definition of a color-adjoint static potential.

III. THE STATIC POTENTIALS ON THE LATTICE

A. Temporal gauge on the lattice

The implementation of temporal gauge in Yang-Mills theory has been worked out a long time ago. The formulation in the continuum based on the Feynman propagation kernel is given in [20,21]. We follow the lattice formulation based on the transfer matrix [22], which is by now textbook standard [23,24].

Temporal gauge $A_0^g = 0$ in the continuum corresponds to temporal links $U_0^g(t, \mathbf{x}) = 1$ on a lattice. These links gauge transform according to

$$U_0^g(t, \mathbf{x}) = g(t, \mathbf{x}) U_0(t, \mathbf{x}) g^\dagger(t + a, \mathbf{x}), \tag{8}$$

where $g(t, \mathbf{x}) \in \mathrm{SU}(N)$. On a lattice with finite temporal extent T with periodic boundary conditions, it is not possible to realize temporal gauge everywhere, since gauge-fixed links must not form closed loops. There will, hence, be one slice of links where $U_0 \neq 1$. Moreover, integration over these unfixed links represents the projection on the charge sectors in Eqs. (32)–(35) below and serves to implement Gauss's law in the path integral formulation [25]. In the following we take $U_0^g(t = 0, \mathbf{x}) \neq 1$ while $U_0^g(t = a.....T - a, \mathbf{x}) = 1$. A possible choice for the gauge transformation $g(t, \mathbf{x})$ implementing temporal gauge is

$$\begin{aligned} g(t = 2a, \mathbf{x}) &= U_0(t = a, \mathbf{x}), \\ g(t = 3a, \mathbf{x}) &= g(t = 2a, \mathbf{x}) U_0(t = 2a, \mathbf{x}) \\ &= U_0(t = a, \mathbf{x}) U_0(t = 2a, \mathbf{x}), \\ g(t = 4a, \mathbf{x}) &= g(t = 3a, \mathbf{x}) U_0(t = 3a, \mathbf{x}) \\ &= U_0(t = a, \mathbf{x}) U_0(t = 2a, \mathbf{x}) U_0(t = 3a, \mathbf{x}), \\ \ldots &= \ldots . \end{aligned} \tag{9}$$

Note that this does not fix the gauge completely, i.e. there are residual time-independent gauge transformations $g(\mathbf{x})$ that preserve the gauge condition $U_0^g(t = a.....T - a, \mathbf{x}) = 1$.

1. The singlet correlator

The trial state $|\Phi^1(\mathbf{x}, \mathbf{x}_0, \mathbf{y})\rangle$ is gauge invariant and so is the corresponding observable, the standard Wilson loop $W_1(r, \Delta t)$. Therefore, its value is identical with or without gauge fixing. For the following, however, it is instructive to consider the gauge-dependent correlator of two spatial strings,

$$\langle \mathrm{Tr}(U(t_1; \mathbf{x}, \mathbf{y}) U(t_2; \mathbf{y}, \mathbf{x})) \rangle, \tag{10}$$

which vanishes without gauge fixing. On the other hand, in temporal gauge it is nonzero and indeed equivalent to the manifestly gauge invariant Wilson loop, as can be seen by writing out the gauge fixed link. In the following we consider two cases.

In case (A) the strings are correlated within the temporal lattice extent, i.e. $a \leq t_1 < t_2 < T$, and we define $\Delta t \equiv t_2 - t_1$ (cf. Fig. 2, left top),

$$\begin{aligned} \langle \mathrm{Tr}(U^g(t_1; \mathbf{x}, \mathbf{y}) U^g(t_2; \mathbf{y}, \mathbf{x})) \rangle_{\text{temporal gauge}} &= \langle \mathrm{Tr}(U(t_1; \mathbf{x}, \mathbf{y}) \underbrace{g^\dagger(t_1, \mathbf{y}) g(t_2, \mathbf{y})}_{= U(t_1, t_2; \mathbf{y})} \\ &\quad \times U(t_2; \mathbf{y}, \mathbf{x}) \underbrace{g^\dagger(t_2, \mathbf{x}) g(t_1, \mathbf{x})}_{= U(t_2, t_1; \mathbf{x})}) \rangle = N \langle W_1(r, \Delta t) \rangle. \end{aligned} \tag{11}$$

In case (B) the correlation is through the periodic temporal boundary, $0 = t_1 < t_2 < T$ (where we define $\Delta t \equiv t_2 - t_1$) or $a \leq t_2 < t_1 < T$ [where we define $\Delta t \equiv t_2 - (t_1 - T)$], cf. Fig. 2 (left bottom). The correlator now includes the unfixed temporal links and in temporal gauge is again equivalent to the gauge invariant Wilson loop, which in this case closes through the boundary,

$$\langle \mathrm{Tr}(U^g(t_1; \mathbf{x}, \mathbf{y}) U_0^g(t = 0, \mathbf{y}) U^g(t_2; \mathbf{y}, \mathbf{x}) (U_0^g)^\dagger (t = 0, \mathbf{x})) \rangle_{\text{temporal gauge}} = N \langle W_1(r, \Delta t) \rangle. \tag{12}$$

Thus, temporal gauge turns a gauge-dependent observable into a gauge invariant observable by implicitly saturating all color charges with static sources, thus ensuring gauge covariant time evolution of the charges. The same observation will in the following be helpful to interpret the color-adjoint static potential.

2. The adjoint correlator

Again we distinguish the cases (A) and (B), which this time yield different results.

Case (A): $a \leq t_1 < t_2 < T$

In temporal gauge the correlator of two spatial strings with additional adjoint transformation behavior at $\mathbf{x}_0$ is equivalent to our observable of interest, the Wilson loop $\langle W_{T^a}(r, \Delta t)\rangle$. Moreover, in temporal gauge both are equivalent to a manifestly gauge invariant observable, as we now show, using the identity

$$\sum_a T^a_{\alpha\beta} T^a_{\gamma\delta} = \frac{1}{2}\left(\delta_{\alpha\delta}\delta_{\beta\gamma} - \frac{1}{N}\delta_{\alpha\beta}\delta_{\gamma\delta}\right). \tag{13}$$

In the following set of equations, the repeated color index a is *not* summed over,

$$\begin{aligned}
&\langle \mathrm{Tr}(U^{T^a,g}(t_1;\mathbf{x},\mathbf{y})U^{(T^a)^\dagger,g}(t_2;\mathbf{y},\mathbf{x}))\rangle_{\text{temporal gauge}} \\
&\quad = N\langle W_{T^a}(r,\Delta t)\rangle_{\text{temporal gauge}} \\
&\quad = \frac{1}{N^2-1}\sum_a \langle \mathrm{Tr}(U(t_1;\mathbf{x},\mathbf{x}_0)g^\dagger(t_1,\mathbf{x}_0)T^a g(t_1,\mathbf{x}_0)U(t_1;\mathbf{x}_0,\mathbf{y})\underbrace{g^\dagger(t_1,\mathbf{y})g(t_2,\mathbf{y})}_{=U(t_1,t_2;\mathbf{y})} \\
&\qquad \times U(t_2;\mathbf{y},\mathbf{x}_0)g^\dagger(t_2,\mathbf{x}_0)\underbrace{(T^a)^\dagger}_{=T^a} g(t_2,\mathbf{x}_0)U(t_2;\mathbf{x}_0,\mathbf{x})\underbrace{g^\dagger(t_2,\mathbf{x})g(t_1,\mathbf{x})}_{=U(t_2,t_1;\mathbf{x})})\rangle \\
&\quad = \frac{1}{2(N^2-1)}\underbrace{\langle \mathrm{Tr}(U(t_1;\mathbf{x},\mathbf{x}_0)\underbrace{g^\dagger(t_1,\mathbf{x}_0)g(t_2,\mathbf{x}_0)}_{=U(t_1,t_2;\mathbf{x}_0)}U(t_2;\mathbf{x}_0,\mathbf{x})U(t_2,t_1;\mathbf{x}))}_{\equiv NW^L(|\mathbf{x}-\mathbf{x}_0|,\Delta t)} \\
&\qquad \underbrace{\times \mathrm{Tr}(U(t_1;\mathbf{x}_0,\mathbf{y})U(t_1,t_2;\mathbf{y})U(t_2;\mathbf{y},\mathbf{x}_0)\underbrace{g^\dagger(t_2,\mathbf{x}_0)g(t_1,\mathbf{x}_0)}_{=U(t_2,t_1;\mathbf{x}_0)}))\rangle}_{\equiv NW^R(|\mathbf{y}-\mathbf{x}_0|,\Delta t)} \\
&\qquad - \frac{1}{2N(N^2-1)}\langle \mathrm{Tr}(U(t_1;\mathbf{x},\mathbf{x}_0)\underbrace{g^\dagger(t_1,\mathbf{x}_0)g(t_1,\mathbf{x}_0)}_{=1}U(t_1;\mathbf{x}_0,\mathbf{y})U(t_1,t_2;\mathbf{y}) \\
&\qquad \times U(t_2;\mathbf{y},\mathbf{x}_0)\underbrace{g^\dagger(t_2,\mathbf{x}_0)g(t_2,\mathbf{x}_0)}_{=1}U(t_2;\mathbf{x}_0,\mathbf{x})U(t_2,t_1;\mathbf{x}))\rangle \\
&= \frac{1}{2(N^2-1)}(N^2\langle W^L(|\mathbf{x}-\mathbf{x}_0|,\Delta t)W^R(|\mathbf{y}-\mathbf{x}_0|,\Delta t)\rangle - \langle W_1(r,\Delta t)\rangle).
\end{aligned} \tag{14}$$

The resulting gauge invariant combination of loops (W^L and W^R denote the left and the right Wilson loop of half size, respectively) is depicted in Fig. 2 [adjoint case (A)]. For an interpretation, it is better to rewrite it more compactly by using the identity (13) twice

$$\langle W_{T^a}(r,\Delta t)\rangle_{\text{temporal gauge}} = \frac{2}{N(N^2-1)}\sum_a\sum_b \langle \mathrm{Tr}(T^a U_R T^b U_L)\mathrm{Tr}(T^a U(t_1,t_2;\mathbf{x}_0)T^b U(t_2,t_1;\mathbf{x}_0))\rangle \tag{15}$$

with the left and right half of the loop

$$U_L \equiv U(t_2;\mathbf{x}_0,\mathbf{x})U(t_2,t_1;\mathbf{x})U(t_1;\mathbf{x},\mathbf{x}_0) \tag{16}$$

$$U_R \equiv U(t_1;\mathbf{x}_0,\mathbf{y})U(t_1,t_2;\mathbf{y})U(t_2;\mathbf{y},\mathbf{x}_0). \tag{17}$$

On the right side the first trace is our observable of interest, the Wilson loop with generator matrix insertions, which now gets multiplied with the adjoint representation of a temporal Wilson line at $\mathbf{x}_0$ (second trace). The latter corresponds to a propagator of a static quark in the adjoint representation. Hence, the gauge invariant expression on the right side is the

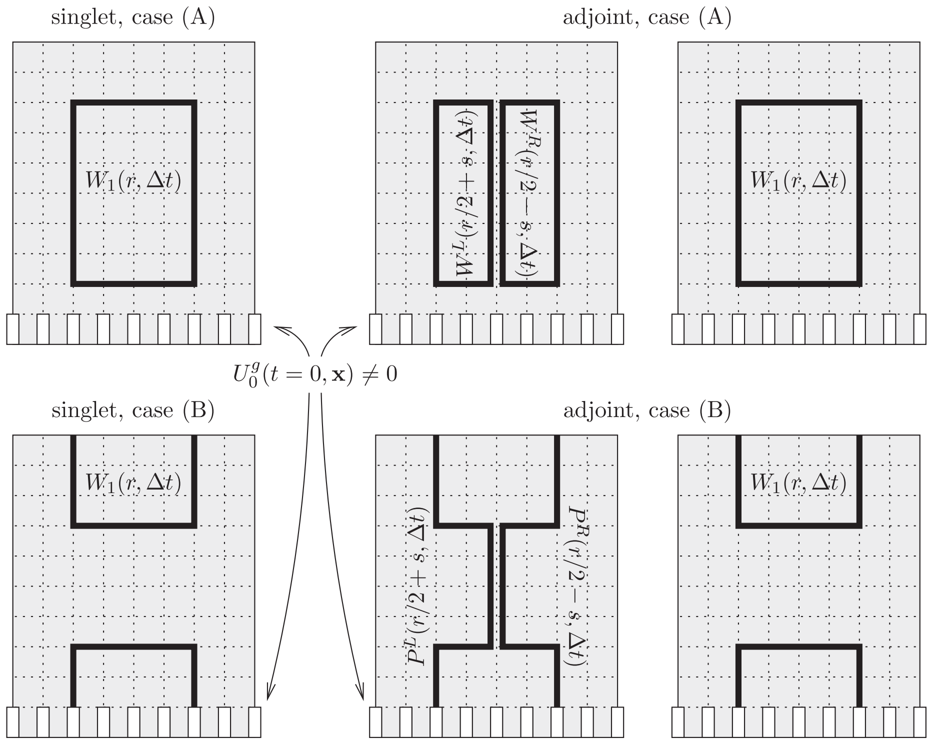

FIG. 2. Gauge invariant observables corresponding to the gauge variant correlators defined in Sec. IIIA1 and IIIA2 in temporal gauge.

correlation function of a gauge invariant three-quark state, one fundamental static quark at $\mathbf{y}$, one fundamental static antiquark at $\mathbf{x}$, one adjoint static quark at $\mathbf{x}_0$. Indeed, after defining

$$|\Phi^{Q\bar{Q}Q^{\mathrm{ad}}}(\mathbf{x}, \mathbf{x}_0, \mathbf{y})\rangle \equiv Q^{\mathrm{ad},a}(\mathbf{x}_0)(\bar{Q}(\mathbf{x})U^{T^a}(\mathbf{x}, \mathbf{y})Q(\mathbf{y}))|0\rangle \tag{18}$$

$$\langle\Phi^{Q\bar{Q}Q^{\mathrm{ad}}}(t_2; \mathbf{x}, \mathbf{x}_0, \mathbf{y})|\Phi^{Q\bar{Q}Q^{\mathrm{ad}}}(t_1; \mathbf{x}, \mathbf{x}_0, \mathbf{y})\rangle \equiv e^{-(2M+M_{\mathrm{ad}})\Delta t}\frac{N(N^2-1)}{2}\langle W_{Q\bar{Q}Q^{\mathrm{ad}}}(r, \Delta t)\rangle, \tag{19}$$

where $U^{T^a}(\mathbf{x}, \mathbf{y})$ has been defined in (3) and M_{ad} denotes the mass of the adjoint static quark, it is easy to verify explicitly that

$$2N\langle W_{T^a}(r, \Delta t)\rangle_{\text{temporal gauge}} = \langle W_{Q\bar{Q}Q^{\mathrm{ad}}}(r, \Delta t)\rangle. \tag{20}$$

Consequently, the static potential $V^{T^a}(r)$ in temporal gauge should not be interpreted as the potential of a static quark and a static antiquark, which form a color-adjoint state. $V^{T^a}(r)$ is rather a potential of a color-singlet three-quark state (one fundamental static quark, one fundamental static antiquark, one adjoint static quark). Note that the potential does not only depend on the $Q\bar{Q}$ separation $r = |\mathbf{x} - \mathbf{y}|$, but also on the position $\mathbf{x}_0$ of the static adjoint quark Q^{ad}. If $\mathbf{x}$, $\mathbf{y}$ and $\mathbf{x}_0$ are on a straight line, the position of the static adjoint quark can be represented by a single parameter $s \equiv |\mathbf{x} - \mathbf{x}_0|/2 - |\mathbf{y} - \mathbf{x}_0|/2$, which is the separation of Q^{ad} from the centre of mass $(\mathbf{x} + \mathbf{y})/2$ of the two fundamental quarks, i.e. $V^{T^a}(r, s)$. This should be kept in mind, while in the following we work with the symmetric alignment $s = 0$.

Case (B): $0 = t_1 < t_2 < T$ or $a \leq t_2 < t_1 < T$

Proceeding as in Sec. IIIA1 for case (B) and in (14) one obtains

$$\langle\mathrm{Tr}(U^{T^a,g}(t_1; \mathbf{x}, \mathbf{y})U_0^g(t = 0, \mathbf{y})\tilde{U}^{(T^a)^\dagger,g}(t_2; \mathbf{y}, \mathbf{x})(U_0^g)^\dagger(t = 0, \mathbf{x}))\rangle_{\text{temporal gauge}} = \frac{1}{2(N^2-1)}(N^2\langle P^L(r/2 + s, \Delta t)P^R(r/2 - s, \Delta t)\rangle - \langle W_1(r, \Delta t)\rangle), \tag{21}$$

which is shown and where $P^L(r/2 + s, \Delta t)$ and $P^R(r/2 - s, \Delta t)$ are defined in Fig. 2 (right bottom).

This correlation function is not suitable, to determine the potential of a static quark and antiquark, which form a color-adjoint state. It contains information about static color-singlet quark-antiquark states propagating through the periodic boundary, and about gluelump states (a static adjoint quark and gluons forming a color-singlet) propagating within the temporal lattice extent. We will explicitly prove this statement using the transfer matrix formalism in Sec. IIIA5.

3. The transfer matrix formalism

A useful theoretical tool to understand which states contribute to a correlation function is the transfer matrix formalism (cf. e.g. [14,26]). The transfer matrix propagates states by one lattice unit in time. In temporal gauge the transfer matrix $\hat{T}_0$ is defined via

$$\langle U_j(t+a)|\hat{T}_0|U_j(t)\rangle \equiv T_{0,t+a\leftrightarrow t}, \quad T_{0,t+a\leftrightarrow t} \equiv e^{-S(U_j(t+a),1,U_j(t))}, \tag{22}$$

where $U_j(t)$ denotes the spatial links of time slice t, $|U_j(t)\rangle$ is the analogue of a position eigenstate in quantum mechanics, i.e. a state with spatial links $U_j(t)$, and

$$S(U_j(t+a),U_0(t),U_j(t)) \equiv \frac{1}{2}S_1(U_j(t+a)) + S_2(U_j(t+a),U_0(t),U_j(t)) + \frac{1}{2}S_1(U_j(t)) \tag{23}$$

$$S_1(U_j(t)) \equiv -\frac{\beta}{2}\sum_{p\in P_t}\mathrm{Re}(\mathrm{Tr}(U_p)) \tag{24}$$

$$S_2(U_j(t+a),U_0(t),U_j(t)) \equiv -\frac{\beta}{2}\sum_{p\in P_{t+a,t}}\mathrm{Re}(\mathrm{Tr}(U_p)) \tag{25}$$

(P_t are spacelike plaquettes on time slice t and $P_{t+a,t}$ are timelike plaquettes connecting time slices t and $t+a$), i.e. $S(U_j(t+a),U_0(t),U_j(t))$ is that part of the lattice Yang-Mills action containing and connecting time slices t and $t+a$ (cf. e.g. [23]).

The transfer matrix $\hat{T}_0$ acts on the Hilbert space of square integrable wave functions, including ones transforming nontrivially under the residual time-independent gauge transformations $g(\mathbf{x})$. The Hilbert space splits into orthogonal sectors with charges in arbitrary representations at any lattice point. Each charge sector can be isolated by appropriate projection operators. Let $\hat{R}[g]$ be an operator to impose a gauge transformation with gauge function $g(\mathbf{x})$,

$$\hat{R}[g]|\psi[U]\rangle = |\psi^g[U]\rangle = |\psi[U^g]\rangle. \tag{26}$$

The transfer matrix in temporal gauge commutes with time-independent gauge transformations, $[\hat{T}_0,\hat{R}[g]]=0$, which implies gauge invariance of its eigenvalues. Another consequence is that eigenstates of $\hat{T}_0$ can simultaneously be chosen as eigenstates of $\hat{R}[g]$, i.e. they can be classified according to irreducible SU(N) color multiplets at each $\mathbf{x}$. For example, for the gauge group $SU(2)$ these have the same structure as spin/angular momentum multiplets, which are well known from ordinary quantum mechanics.

Specifically, we list the transformation behavior of states occurring in our analysis: (i) color singlets, (ii) states with a fundamental charge at $\mathbf{y}$ and an antifundamental one at $\mathbf{x}$, (iii) states with an adjoint charge at $\mathbf{x}_0$ and finally (iv) states with a fundamental charge at $\mathbf{y}$, an antifundamental one at $\mathbf{x}$ and an adjoint charge at $\mathbf{x}_0$,

$$\text{(i) } \hat{R}[g]|\psi\rangle = |\psi\rangle \tag{27}$$

$$\text{(ii) } \hat{R}[g]|\psi_{\alpha\beta}\rangle = g_{\alpha\gamma}(\mathbf{x})g^\dagger_{\delta\beta}(\mathbf{y})|\psi_{\gamma\delta}\rangle \tag{28}$$

$$\text{(iii) } \hat{R}[g]|\psi^a\rangle = D^A_{ab}(g(\mathbf{x}_0))|\psi^b\rangle \tag{29}$$

$$\text{(iv) } \hat{R}[g]|\psi^a_{\alpha\beta}\rangle = g_{\alpha\gamma}(\mathbf{x})g^\dagger_{\delta\beta}(\mathbf{y})D^A_{ab}(g(\mathbf{x}_0))|\psi^b_{\gamma\delta}\rangle, \tag{30}$$

where $D^A_{ab}(g)$ are the representation matrices of the adjoint representation,

$$D^A_{ab}(g) = 2\mathrm{Tr}(g^\dagger T^a g T^b). \tag{31}$$

The projectors onto the corresponding orthogonal charge sectors of the Hilbert space are

$$\text{(i) } \hat{P} = \int Dg\hat{R}[g] \tag{32}$$

$$\text{(ii) } \hat{P}^{F\otimes\bar{F}}_{\alpha\beta\mu\nu} = \int Dg g^\dagger_{\alpha\beta}(\mathbf{x})g_{\mu\nu}(\mathbf{y})\hat{R}[g] \tag{33}$$

$$\text{(iii) } \hat{P}^A_{ab} = \int Dg D^A_{ab}(g^\dagger(\mathbf{x}_0))\hat{R}[g] \tag{34}$$

$$\text{(iv) } \hat{P}^{F\otimes\bar{F}\otimes A}_{\alpha\beta\mu\nu ab} = \int Dg g^\dagger_{\alpha\beta}(\mathbf{x})g_{\mu\nu}(\mathbf{y})D^A_{ab}(g^\dagger(\mathbf{x}_0))\hat{R}[g]. \tag{35}$$

For example, (ii) maps the component $|\psi_{\beta\mu}\rangle$ of a representation $F\otimes\bar{F}$ to the component $|\psi_{\alpha\nu}\rangle$ and annihilates all other components and charge sectors.[1] Direct calculation shows

$$\hat{P}^{F\otimes\bar{F}}_{\alpha\beta\mu\nu}|\psi_{\gamma\delta}\rangle = \frac{1}{N^2}\delta_{\beta\gamma}\delta_{\mu\delta}|\psi_{\alpha\nu}\rangle, \quad \hat{P}^{F\otimes\bar{F}}_{\alpha\beta\mu\nu}|\psi_{\beta\mu}\rangle = |\psi_{\alpha\nu}\rangle. \tag{36}$$

Similarly, one verifies

[1] This is due to the fact that only group integrals over the trivial representation are nonzero [27], $\int Dg = 1$, $\int Dg g_{\alpha\beta} = 0$, $\int dg g_{ij} g^\dagger_{kl} = (1/N)\delta_{il}\delta_{jk}, \ldots$.

$$\hat{P}^{\mathrm{F}\otimes\bar{\mathrm{F}}\otimes A}_{\alpha\beta\mu\nu ab}|\psi^{c}_{\gamma\delta}\rangle = \frac{1}{N^2(N^2-1)}\delta_{\beta\gamma}\delta_{\mu\delta}\delta_{bc}|\psi^{a}_{\alpha\nu}\rangle,$$
$$\hat{P}^{\mathrm{F}\otimes\bar{\mathrm{F}}\otimes A}_{\alpha\beta\mu\nu ab}|\psi^{b}_{\beta\mu}\rangle = |\psi^{a}_{\alpha\nu}\rangle. \tag{37}$$

4. Spectral analysis of Wilson loops, case (A)

We are now ready to perform the spectral analysis of our lattice observables in temporal gauge. We start by considering those observables, where the corresponding Wilson loops do not include links $U_0(t=0,\mathbf{x}) \neq 1$ [cf. Fig. 2, singlet, case (A) and adjoint, case (A)]. To this end we write out the Euclidean path integral in terms of the transfer matrix,

$$N\langle W_\Sigma(r,\Delta t)\rangle = \frac{1}{Z}\int DU_j \int DU_0(0) U^{\Sigma}_{\alpha\beta}(t_1;\mathbf{x},\mathbf{y}) \times U^{\Sigma^\dagger}_{\beta\alpha}(t_2;\mathbf{y},\mathbf{x})$$
$$T_{0,0\leftrightarrow T-a}\ldots T_{0,3a\leftrightarrow 2a}T_{0,2a\leftrightarrow a}e^{-S(U_j(a),U_0(0),U_j(0))}, \tag{38}$$

where $\int DU_j$ denotes the integration over all spatial links and $\int DU_0(0)$ the integration over all temporal links connecting time slice $t=0$ and $t=a$. The path integral can now be rewritten according to

$$\begin{aligned} N\langle W_\Sigma(r,\Delta t)\rangle &= \frac{1}{Z}\int DU_j \int Dg U^{\Sigma}_{\alpha\beta}(t_1;\mathbf{x},\mathbf{y})U^{\Sigma^\dagger}_{\beta\alpha}(t_2;\mathbf{y},\mathbf{x}) \times T_{0,0\leftrightarrow T-a}\ldots T_{0,2a\leftrightarrow a}e^{-S(U_j(a),1,U^{g^\dagger}_j(0))} \\ &= \frac{1}{Z}\mathrm{Tr}(\hat{T}_0^{T-t_2}\hat{U}^{\Sigma^\dagger}_{\beta\alpha}(\mathbf{y},\mathbf{x})\hat{T}_0^{t_2-t_1}\hat{U}^{\Sigma}_{\alpha\beta}(\mathbf{x},\mathbf{y})\hat{T}_0^{t_1}\hat{P}) \\ &= \frac{1}{Z}\sum_{k,m,n}\langle n|\hat{T}_0^{T-t_2}\hat{U}^{\Sigma^\dagger}_{\beta\alpha}(\mathbf{y},\mathbf{x})|k\rangle\langle k|\hat{T}_0^{t_2-t_1}\hat{U}^{\Sigma}_{\alpha\beta}(\mathbf{x},\mathbf{y})|m\rangle\langle m|\hat{T}_0^{t_1}\hat{P}|n\rangle \\ &= \frac{1}{Z}\sum_{k,m,n}e^{-E_n(T-t_2)}e^{-E_k(t_2-t_1)}e^{-E_m t_1}\times\langle n|(\hat{U}^{\Sigma}_{\alpha\beta}(\mathbf{x},\mathbf{y}))^\dagger|k\rangle\langle k|\hat{U}^{\Sigma}_{\alpha\beta}(\mathbf{x},\mathbf{y})|m\rangle\langle m|\hat{P}|n\rangle. \end{aligned} \tag{39}$$

$\hat{P}|n\rangle \neq 0$ only, if $|n\rangle$ is a gauge invariant state, i.e. if $|n\rangle$ is a color-singlet. Then $\langle m|\hat{P}|n\rangle = \delta_{mn}$ and

$$N\langle W_\Sigma(r,\Delta t)\rangle = \frac{1}{Z}\sum_{k,n'}e^{-E_k\Delta t}e^{-E_{n'}(T-\Delta t)} \times\sum_{\alpha,\beta}|\langle k|\hat{U}^{\Sigma}_{\alpha\beta}(\mathbf{x},\mathbf{y})|n'\rangle|^2, \tag{40}$$

where $\sum_{n'}$ is over gauge invariant states $|n'\rangle$ only. The nature of the states $|k\rangle$ is determined by the choice of Σ.

For $\Sigma = 1$ the state $\hat{U}^{\Sigma}_{\alpha\beta}(\mathbf{x},\mathbf{y})|n'\rangle = \hat{U}_{\alpha\beta}(\mathbf{x},\mathbf{y})|n'\rangle$ transforms under gauge transformations according to (28). Hence,

$$\langle k|\hat{U}_{\alpha\beta}(\mathbf{x},\mathbf{y})|n'\rangle = \langle k|\hat{P}^{\mathrm{F}\otimes\bar{\mathrm{F}}}_{\alpha\mu\nu\beta}\hat{U}_{\mu\nu}(\mathbf{x},\mathbf{y})|n'\rangle \tag{41}$$

such that only states $\langle k'_{\alpha\beta}|$ with the same transformation behavior contribute to the sum, while all others are annihilated,

$$N\langle W_1(r,\Delta t)\rangle = \frac{1}{Z}\sum_{k',n'}e^{-V^1_{k'}(r)\Delta t}e^{-\mathcal{E}_{n'}(T-\Delta t)} \times\sum_{\alpha,\beta}|\langle k'_{\alpha\beta}|\hat{U}_{\alpha\beta}(\mathbf{x},\mathbf{y})|n'\rangle|^2 \tag{42}$$

($\mathcal{E}_{n'}$ denotes eigenvalues of gauge invariant eigenstates of $\hat{T}_0$, i.e. states without static quarks). Using the spectral decomposition of the partition function,

$$Z = \sum_{k'}e^{-\mathcal{E}_{k'}T}, \tag{43}$$

and considering infinite temporal lattice extent reduces $\sum_{n'}$ to the vacuum,

$$\begin{aligned} N\langle W_1(r,\Delta t)\rangle &= \frac{\sum_{k',n'}e^{-V^1_{k'}(r)\Delta t}e^{-\mathcal{E}_{n'}(T-\Delta t)}\sum_{\alpha,\beta}|\langle k'_{\alpha\beta}|\hat{U}_{\alpha\beta}(\mathbf{x},\mathbf{y})|n'\rangle|^2}{\sum_{k'}e^{-\mathcal{E}_{k'}T}} \\ &\overset{T\to\infty}{=} \sum_{k'}e^{-(V^1_{k'}(r)-\mathcal{E}_0)\Delta t}\sum_{\alpha,\beta}|\langle k'_{\alpha\beta}|\hat{U}_{\alpha\beta}(\mathbf{x},\mathbf{y})|0\rangle|^2. \end{aligned} \tag{44}$$

This is of course the well-known result for the color-singlet static potential. Note that there is a sum over α and β in (42) and (44), which is a sum over the N^2 possible color orientations of the static quark and the static antiquark. Both the eigenvalues of the transfer matrix $V^1_{k'}(r)$ and the corresponding matrix elements $|\langle k'_{\alpha\beta}|\hat{U}_{\alpha\beta}(\mathbf{x},\mathbf{y})|n'\rangle|^2$ (no sum over α and β) are independent of α and β, i.e. each quark-antiquark color orientation yields the same contribution to the correlation function. In other words in temporal gauge the color orientations of the static quark and the static antiquark are irrelevant, i.e. any color orientation will result in the singlet static potential.

The result for the color-adjoint case, i.e. $\Sigma = T^a$, follows in complete analogy. In this case the state $\hat{U}^{\Sigma}_{\alpha\beta}(\mathbf{x},\mathbf{y})|n'\rangle = \hat{U}^{T^a}_{\alpha\beta}(\mathbf{x},\mathbf{y})|n'\rangle$ transforms as in (30) and we have

$$\langle k|\hat{U}^{T^a}_{\alpha\beta}(\mathbf{x},\mathbf{y})|n'\rangle = \langle k|\hat{P}^{\mathrm{F}\otimes\bar{\mathrm{F}}\otimes A}_{\alpha\mu\nu\beta ab}\hat{U}^{b}_{\mu\nu}(\mathbf{x},\mathbf{y})|n'\rangle \tag{45}$$

such that only states $\langle k'^{a}_{\alpha\beta}|$ with the same transformation behavior contribute to the sum. The final result is

$$N\langle W_{T^a}(r,\Delta t)\rangle \overset{T\to\infty}{=} \sum_{k'} e^{-(V^{T^a}_{k'}(r)-\mathcal{E}_0)\Delta t}\sum_{\alpha,\beta}|\langle k'^a_{\alpha\beta}|\hat{U}^a_{\alpha\beta}(\mathbf{x},\mathbf{y})|0\rangle|^2. \quad (46)$$

This correlation function is suited to extract a three-quark potential of a fundamental static quark, a fundamental static antiquark and an adjoint static quark. It is not a quark- antiquark potential with the quark and the antiquark in a color-adjoint orientation, i.e. it should not be interpreted as a color-adjoint static potential. As for $\Sigma = 1$ the potential is independent of the color orientations of the three quarks. Cf. also Sec. IIIA2, where the same result has been obtained using different methods and arguments.

Finally, in the case $\Sigma = T^a\mathbf{B}^a$ the state $\hat{U}^\Sigma_{\alpha\beta}(\mathbf{x},\mathbf{y})|n'\rangle = \hat{U}^{T^a\mathbf{B}^a}_{\alpha\beta}(\mathbf{x},\mathbf{y})|n'\rangle$ again transforms as in (28), i.e. has fundamental charges at $\mathbf{x}$ and $\mathbf{y}$. Hence,

$$\langle k|\hat{U}^{T^a\mathbf{B}^a}_{\alpha\beta}(\mathbf{x},\mathbf{y})|n'\rangle = \langle k|\hat{P}^{\mathrm{F}\otimes\bar{\mathrm{F}}}_{\alpha\mu\nu\beta}\hat{U}^{T^a\mathbf{B}^a}_{\mu\nu}(\mathbf{x},\mathbf{y})|n'\rangle \quad (47)$$

and thus only states $\langle k'_{\alpha\beta}|$ contribute. These are in the same color charge sector as those in (42); however, in this case their parity is negative (for a more detailed discussion regarding quantum numbers [other than color] of states with two static charges we refer to e.g. [28,29]). The final result for this case then reads

$$\langle W_B(r,\Delta t)\rangle \overset{T\to\infty}{\to} \sum_{k'} e^{-(V^{1,-}_{k'}(r)-\mathcal{E}_0)\Delta t}\sum_{\alpha,\beta}|\langle k'_{\alpha\beta}|\hat{U}^{T^a\mathbf{B}^a}_{\alpha\beta}(\mathbf{x};\mathbf{y})|0\rangle|^2. \quad (48)$$

The exponential decay is with color-singlet potentials in the negative parity channel, thus $\langle W_B(r,\Delta t)\rangle$ is not suitable, to define a color-adjoint static potential.

5. Spectral analysis of Wilson loops, case (B)

In this section we give the spectral decomposition for the situation, where the correlators close through the temporal boundary. The backwards Wilson loop, cf. Fig. 2 (left bottom), can be rewritten according to

$$\begin{aligned}
N\langle W^b_1(r,\Delta t)\rangle &= \frac{1}{Z}\int DU_j\int DU_0(0)U^\dagger_{0,\alpha\beta}(t=0,\mathbf{x})U_{\beta\gamma}(t_1;\mathbf{x},\mathbf{y})U_{0,\gamma\delta}(t=0,\mathbf{y})U_{\delta\alpha}(t_2;\mathbf{y},\mathbf{x})\\
&\quad\times T_{0,0\leftrightarrow T-a}\ldots T_{0,3a\leftrightarrow 2a}T_{0,2a\leftrightarrow a}e^{-S(U_j(a),U_0(0),U_j(0))}\\
&= \frac{1}{Z}\int DU_j\int Dg g^\dagger_{\alpha\beta}(\mathbf{x})U_{\beta\gamma}(t_1;\mathbf{x},\mathbf{y})g_{\gamma\delta}(\mathbf{y})U_{\delta\alpha}(t_2;\mathbf{y},\mathbf{x})T_{0,0\leftrightarrow T-a}\ldots T_{0,3a\leftrightarrow 2a}T_{0,2a\leftrightarrow a}e^{-S(U_j(a),1,U^{g^\dagger}_j(0))}\\
&= \frac{1}{Z}\sum_{k,m,n}e^{-E_n(T-t_1)}e^{-E_k(t_1-t_2)}e^{-E_m t_2}\langle n|\hat{U}_{\beta\gamma}(\mathbf{x},\mathbf{y})|k\rangle\langle k|(\hat{U}^\dagger_{\alpha\delta}(\mathbf{x},\mathbf{y}))|m\rangle\langle m|\hat{P}^{\mathrm{F}\otimes\bar{\mathrm{F}}}_{\alpha\beta\gamma\delta}|n\rangle.
\end{aligned} \quad (49)$$

Because of the projector, $\sum_{m,n}$ can be restricted to all eigenstates which transform as in (28) and $\langle m'|n'\rangle = \delta_{m'n'}$. The other matrix elements then require $\hat{U}_{\beta\gamma}(\mathbf{x},\mathbf{y})|k\rangle$ to transform in the same way, which implies $|k\rangle$ to be in the singlet sector. We finally obtain

$$N\langle W^b_1(r,\Delta t)\rangle = \frac{1}{Z}\sum_{k',n'}e^{-V^1_{n'}\Delta t}e^{-\mathcal{E}_{k'}(T-\Delta t)}\sum_{\beta\gamma}|\langle n'_{\beta\gamma}|\hat{U}_{\beta\gamma}(\mathbf{x},\mathbf{y})|k'\rangle|^2. \quad (50)$$

This result is identical to (42), i.e. as expected the position of the Wilson loop relative to the slice of links $U_0(t=0,\mathbf{x}) \neq 1$ does not matter.

Similarly one can study the backwards correlator of the adjoint string $U^{T^a}_{\alpha\beta}(\mathbf{x},\mathbf{y})$, cf. Fig. 2 (right bottom). In this case

$$\begin{aligned}
N\langle W^b_{T^a}(r,\Delta t)\rangle &= \frac{1}{Z}\int DU_j\int DU_0(0)U^\dagger_{0,\alpha\beta}(t=0,\mathbf{x})U^{T^a}_{\beta\gamma}(t_1;\mathbf{x},\mathbf{y})U_{0,\gamma\delta}(t=0,\mathbf{y})U^{(T^a)^\dagger}_{\delta\alpha}(t_2;\mathbf{y},\mathbf{x})\\
&\quad\times T_{0,0\leftrightarrow T-a}\ldots T_{0,3a\leftrightarrow 2a}T_{0,2a\leftrightarrow a}e^{-S(U_j(a),U_0(0),U_j(0))}\\
&= \frac{1}{Z}\sum_{k,m,n}e^{-E_n(T-t_1)}e^{-E_k(t_1-t_2)}e^{-E_m t_2}\langle n|\hat{U}^{T^a}_{\beta\gamma}(\mathbf{x},\mathbf{y})|k\rangle\langle k|(\hat{U}^{T^a}_{\alpha\delta}(\mathbf{x},\mathbf{y}))^\dagger|m\rangle\langle m|\hat{P}^{\mathrm{F}\otimes\bar{\mathrm{F}}}_{\alpha\beta\gamma\delta}|n\rangle\\
&= \frac{1}{N^2 Z}\sum_{k',n'}e^{-V^1_{n'}(r)\Delta t}e^{-\mathcal{E}^{Q^{\mathrm{adj}}}_{k'}T}|\langle n'_{\beta\gamma}|\hat{U}^{T^a}_{\beta\gamma}(\mathbf{x},\mathbf{y})|k'^a\rangle|^2,
\end{aligned} \quad (51)$$

where we have again used that the projector restricts $|m\rangle$ and $|n\rangle$ to states transforming as in (28) and $m' = n'$. Now $(\hat{U}^{T^a}_{\alpha\delta}(\mathbf{x},\mathbf{y}))^\dagger |m'_{\alpha\delta}\rangle$ transforms as in (29), i.e. the states $|k\rangle$ are required to transform as a single adjoint charge at $\mathbf{x}_0$ (the corresponding eigenvalues of the transfer matrix are denoted by $\mathcal{E}^{Q^{\mathrm{adj}}}_{k'}$).

In the limit $T \to \infty$ this simplifies to

$$N\langle W^b_{T^a}(r,\Delta t)\rangle = \sum_{k',n'} e^{-(V^1_{n'}(r)-\mathcal{E}^{Q^{\mathrm{adj}}}_0)\Delta t} e^{-(\mathcal{E}^{Q^{\mathrm{adj}}}_0-\mathcal{E}_0)T} \times \sum_{\beta,\gamma} |\langle n'_{\beta\gamma}|\hat{U}^{T^a}_{\beta\gamma}(\mathbf{x},\mathbf{y})|k'^a\rangle|^2. \quad (52)$$

This correlation function is suited to extract the common singlet potential $V^1(r) = V^1_0(r)$ and a gluelump mass $\mathcal{E}^{Q^{\mathrm{adj}}}_0$. Cf. also Sec. IIIA2, where the same result has been obtained using different methods and arguments.

B. Coulomb gauge on the lattice

Another gauge featuring a transfer matrix/Hamiltonian is Coulomb gauge $\partial_j A^g_j = 0$. On the lattice it corresponds to links $U^g_j(t,\mathbf{x})$, which minimize

$$\sum_{t,\mathbf{x}} \sum_{j=1,2,3} \mathrm{Re}(\mathrm{Tr}(1 - U^g_j(t,\mathbf{x}))) \quad (53)$$

(for more details cf. e.g. [15]).

The gauge invariant color-singlet Wilson loop remains identically the same, which is why we do not discuss it again. Similar to the analysis presented in Sec. IIIA2 one can write the color-adjoint Wilson loop as

$$\begin{aligned}
&\langle W_{T^a}(r,\Delta t)\rangle_{\text{Coulomb gauge}} \\
&= \frac{1}{N}\langle \mathrm{Tr}(T^a U_R T^a U_L)\rangle_{\text{Coulomb gauge}} \\
&= \frac{1}{N}\langle \mathrm{Tr}(T^a g(t_1,\mathbf{x}_0) U_R g^\dagger(t_2,\mathbf{x}_0) T^a g(t_2,\mathbf{x}_0) U_L g^\dagger(t_1,\mathbf{x}_0))\rangle \\
&= \frac{1}{N}\langle \mathrm{Tr}(T^a h^{\mathrm{res}}(t_1) g^{\mathrm{Coulomb}}(t_1,\mathbf{x}_0) \\
&\quad \times U_R g^{\mathrm{Coulomb},\dagger}(t_2,\mathbf{x}_0) h^{\mathrm{res},\dagger}(t_2) T^a h^{\mathrm{res}}(t_2) g^{\mathrm{Coulomb}}(t_2,\mathbf{x}_0) \\
&\quad \times U_L g^{\mathrm{Coulomb},\dagger}(t_1,\mathbf{x}_0) h^{\mathrm{res},\dagger}(t_1))\rangle. \qquad (54)
\end{aligned}$$

Since the Coulomb gauge condition does not fix the gauge completely (a space-independent residual gauge symmetry remains), we have split the gauge transformation according to $g(t,\mathbf{x}) \equiv h^{\mathrm{res}}(t) g^{\mathrm{Coulomb}}(t,\mathbf{x})$, where $g(t,\mathbf{x})^{\mathrm{Coulomb}} \in SU(N)$ transforms the links to Coulomb gauge and $h^{\mathrm{res}}(t) \in SU(N)$ represents the residual gauge degrees of freedom.

Without imposing any additional gauge condition restricting $h^{\mathrm{res}}(t)$ one obtains in a nonperturbative evaluation

$$\langle W_{T^a}(r,\Delta t)\rangle_{\text{Coulomb gauge}} = 0. \quad (55)$$

Because of the integration over $h^{\mathrm{res}}(t)$ the color-adjoint Wilson loop averages to zero (note that, as in the case without gauge fixing, a parallel transport in time between the two generators T^a is missing).

One can complete the gauge fixing by e.g. also requiring $U^g_0(t,\mathbf{z}_0) = 1$, where $\mathbf{z}_0$ is an arbitrary point in space. This condition imposes temporal gauge (cf. Sec. IIIA) to temporal links at $\mathbf{z}_0$. $h^{\mathrm{res}}(t)$ is then chosen as specified by (9), replacing g by h^{res} and $\mathbf{x}$ by $\mathbf{z}_0$. The Wilson loop average is then nonvanishing. Similar to (15) it can be written as

$$\begin{aligned}
\langle W_{T^a}(r,\Delta t)\rangle_{\text{Coulomb gauge}} = \frac{2}{N(N^2-1)} \sum_a \sum_b \langle \mathrm{Tr}(T^a g^{\mathrm{Coulomb}}(t_1,\mathbf{x}_0) U_R g^{\mathrm{Coulomb},\dagger}(t_2,\mathbf{x}_0) T^b g^{\mathrm{Coulomb}}(t_2,\mathbf{x}_0) \\
\times U_L g^{\mathrm{Coulomb},\dagger}(t_1,\mathbf{x}_0)) \mathrm{Tr}(T^a U(t_1,t_2;\mathbf{z}_0) T^b U(t_2,t_1;\mathbf{z}_0))\rangle. \qquad (56)
\end{aligned}$$

The second trace, which arises due to h^{res}, corresponds to a propagator of a static quark in the adjoint representation at $\mathbf{z}_0$. Consequently the color-adjoint static potential in this "completed Coulomb gauge" should also be interpreted as a potential of three static quarks, one fundamental static quark at $\mathbf{y}$, one fundamental static antiquark at $\mathbf{x}$ and one adjoint static quark at $\mathbf{z}_0$. For the choice $\mathbf{z}_0 = \mathbf{x}_0$ the resulting potential agrees with that in temporal gauge (with modified matrix elements). This is clearly not in line with the perturbative result (78), where no adjoint static quark exists. Moreover, note that the color-adjoint static potential in completed Coulomb gauge depends on $\mathbf{z}_0$, which is now part of the gauge condition. Thus, even within this class of gauges the color-adjoint static potential is gauge dependent and depends on the details of the gauge condition.

IV. LEADING-ORDER PERTURBATIVE CALCULATIONS

While some of the following calculations are neither new nor original, we review the leading-order perturbative results for the correlators discussed here in Lorenz as well as in Coulomb gauge.

A. Lorenz gauge

The gluon propagator in Lorenz gauge $\partial_\mu A_\mu = 0$ is

$$D^{ab}_{\mu\nu}(x,y) = \frac{1}{(2\pi)^4}\int d^4p e^{-ip(x-y)} \times \delta^{ab}\frac{1}{p^2}\left(\delta_{\mu\nu} - (1-\xi)\frac{p_\mu p_\nu}{p^2}\right). \quad (57)$$

In the following we use $\xi = 1$ (Feynman gauge), i.e.

$$D^{ab}_{\mu\nu}(x,y) = \delta^{ab}\delta_{\mu\nu}\frac{1}{(2\pi)^4}\int d^4p e^{-ip(x-y)}\frac{1}{p^2} = \delta^{ab}\delta_{\mu\nu}\frac{1}{4\pi^2(x-y)^2}. \quad (58)$$

The perturbative expansion of the Wilson loop (4) with $\Sigma = 1, T^a$ is [cf. Fig. 3(a) and (b)]

$$\begin{aligned}\langle W_\Sigma(r,\Delta t)\rangle &= \left\langle \frac{1}{N}\mathrm{Tr}\left(\Sigma P \exp\left(ig\int_{C_1} dz_\mu A_\mu(z)\right)\Sigma^\dagger P \exp\left(ig\int_{C_2} dz_\nu A_\nu(z)\right)\right)\right\rangle \\ &= \frac{1}{N}\mathrm{Tr}(\Sigma\Sigma^\dagger) - \frac{g^2}{N}\mathrm{Tr}(\Sigma T^a \Sigma^\dagger T^b)\int_{C_1} dx_\mu \int_{C_2} dy_\nu D^{ab}_{\mu\nu}(x,y) \\ &\quad - \frac{g^2}{2N}\mathrm{Tr}(\Sigma T^a T^b \Sigma^\dagger)\int_{C_1} dx_\mu \int_{C_1} dy_\nu D^{ab}_{\mu\nu}(x,y) \\ &\quad - \frac{g^2}{2N}\mathrm{Tr}(\Sigma\Sigma^\dagger T^a T^b)\int_{C_2} dx_\mu \int_{C_2} dy_\nu D^{ab}_{\mu\nu}(x,y) + \mathcal{O}(g^4). \quad (59)\end{aligned}$$

In the limit of interest, $\Delta t \to \infty$, the contribution of the spatial strings is suppressed and the integrals receive contributions from the same temporal parallel transporter,

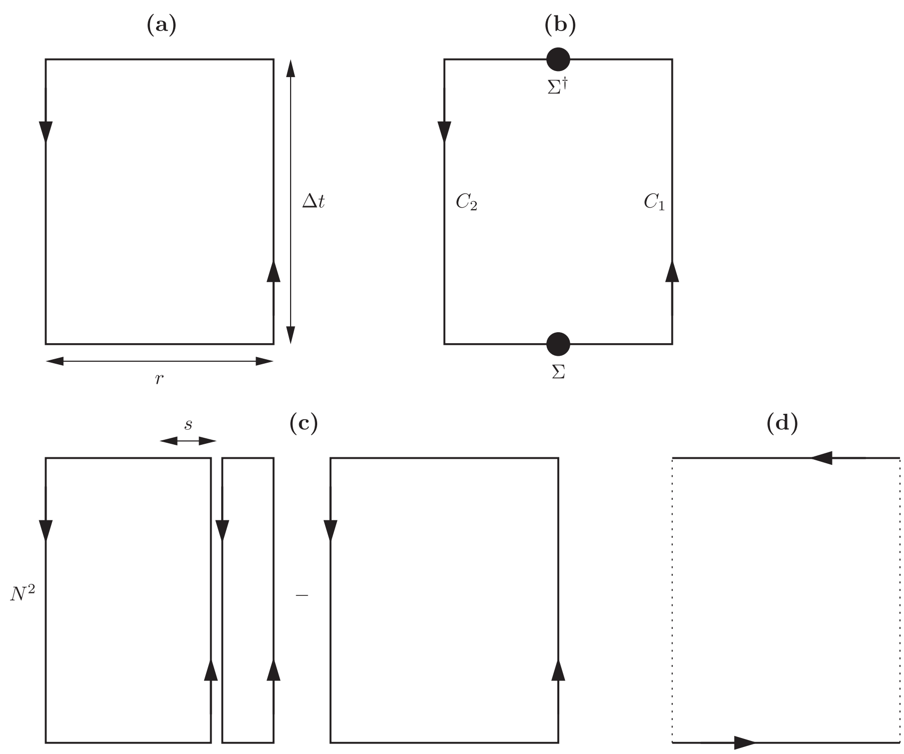

FIG. 3. Loops and diagrams calculated perturbatively in Sec. IV.

$$\lim_{\epsilon\to 0}\int_{-\Delta t/2}^{+\Delta t/2} dt_1 \int_{-\Delta t/2}^{+\Delta t/2} dt_2 \frac{1}{4\pi^2((t_1-t_2)^2+\epsilon^2)} = \frac{1}{4\pi^2}\lim_{\epsilon\to 0}\left(+\frac{2\Delta t}{\epsilon}\arctan(\Delta t/\epsilon) - \ln\left(\frac{\Delta t^2}{\epsilon^2}\right)\right) = \frac{1}{4\pi^2}\lim_{\epsilon\to 0}\left(+\frac{\pi\Delta t}{\epsilon} - \ln\left(\frac{\Delta t^2}{\epsilon^2}\right)\right), \quad (60)$$

or from opposite temporal parallel transporters,

$$\int_{-\Delta t/2}^{+\Delta t/2} dt_1 \int_{+\Delta t/2}^{-\Delta t/2} dt_2 \frac{1}{4\pi^2((t_1-t_2)^2+r^2)} = \frac{1}{4\pi^2}\left(-\frac{2\Delta t}{r}\arctan(\Delta t/r) + \ln\left(\frac{\Delta t^2+r^2}{r^2}\right)\right). \quad (61)$$

One thus obtains

$$\lim_{\Delta t\to\infty}\langle W_\Sigma(r,\Delta t)\rangle = \frac{1}{N}\mathrm{Tr}(\Sigma\Sigma^\dagger) - g^2\left(C(\Sigma) - \frac{\mathrm{Tr}(\Sigma T^a\Sigma^\dagger T^a)}{4N\pi r}\right)\Delta t + \mathcal{O}(g^4), \quad (62)$$

where $C(\Sigma)$ is an infinite constant, i.e. independent of r.

We begin by discussing the standard Wilson loop, $\Sigma = 1$. In this case $\mathrm{Tr}(\Sigma\Sigma^\dagger) = N$ and $\mathrm{Tr}(\Sigma T^a \Sigma^\dagger T^a) = (N^2-1)/2$. In Lorenz gauge a transfer matrix or Hamiltonian does not exist. However, for the manifestly gauge invariant Wilson loop the time evolution is the same in any gauge and without gauge fixing. Therefore, for large temporal separations Δt they are guaranteed to decay exponentially proportional to the eigenvalue of the lowest energy eigenstate with corresponding quantum numbers,

$$\lim_{\Delta t\to\infty}\langle W_\Sigma(r,\Delta t)\rangle = A\exp(-V^\Sigma(r)\Delta t) = A\exp(-(V^{\Sigma,(0)} + g^2 V^{\Sigma,(2)}(r) + \mathcal{O}(g^4))\Delta t) = A\exp(-V^{\Sigma,(0)}\Delta t)\exp(-(g^2V^{\Sigma,(2)}(r)+\mathcal{O}(g^4))\Delta t) = A\exp(-V^{\Sigma,(0)}\Delta t)(1 - g^2V^{\Sigma,(2)}(r)\Delta t + \mathcal{O}(g^4)), \quad (63)$$

where $V^{\Sigma,(n)}(r)$ denote those terms of $V^\Sigma(r)$, which are proportional to g^n, i.e. $V^\Sigma(r) = V^{\Sigma,(0)} + g^2V^{\Sigma,(2)}(r) + \mathcal{O}(g^4)$. Comparing powers of g^2 in (62) and (63) yields the singlet static potential,

$$V^1(r) = -\frac{(N^2-1)g^2}{8N\pi r} + \mathrm{const} + \mathcal{O}(g^4). \quad (64)$$

For the adjoint case $\Sigma = T^a$ and without summing over a we have $\mathrm{Tr}(\Sigma\Sigma^\dagger) = 1/2$ and $\mathrm{Tr}(\Sigma T^a\Sigma^\dagger T^a) = -1/4N$. Assuming exponential decay as above and comparing powers of g^2 one finds the result known in the literature,

$$V^{T^a}(r) = +\frac{g^2}{8N\pi r} + \mathrm{const} + \mathcal{O}(g^4). \quad (65)$$

Note that (65) is independent of the position of Σ, i.e. independent of s. However, since in Lorenz gauge a transfer matrix or Hamiltonian does not exist, the exponential form of (63) only holds for manifestly gauge invariant observables like the ordinary Wilson loop. By contrast, in the limit of large Δt the correlator $\langle W_{T^a}(r,\Delta t)\rangle$ in Lorenz gauge is neither positive nor exponentially decaying. In other words, the physical meaning of the result (65), which often appears in the literature, is unclear.

The importance of a gauge-covariant time evolution of color charges by means of parallel transport is highlighted by the perturbative evaluation of the string-string correlator (10) in Lorenz gauge,

$$\begin{aligned}\frac{1}{N}\langle\mathrm{Tr}(U(t_1;\mathbf{x},\mathbf{y})U(t_2;\mathbf{y},\mathbf{x}))\rangle_{\text{Lorenz gauge}} &= \frac{1}{N}\left\langle\mathrm{Tr}\left(P\exp\left(ig\int_{-r/2}^{+r/2}dzA_3(-\Delta t/2,0,0,z)\right)\right.\right. \\ &\quad\left.\left.\times P\exp\left(ig\int_{+r/2}^{-r/2}dzA_3(+\Delta t/2,0,0,z)\right)\right)\right\rangle_{\text{Lorenz gauge}} \\ &= 1 - \frac{(N^2-1)g^2}{8N\pi^2}\left(\lim_{\varepsilon\to 0}\left(+\frac{\pi r}{\varepsilon} - \ln\left(\frac{r^2}{\varepsilon^2}\right)\right) - \frac{2r}{\Delta t}\arctan(r/\Delta t) + \ln\left(\frac{\Delta t^2+r^2}{\Delta t^2}\right)\right) \\ &\quad + \mathcal{O}(g^4) \\ &\overset{\Delta t\to\infty}{\to} 1 - \frac{(N^2-1)g^2}{8N\pi^2}\left(\lim_{\varepsilon\to 0}\left(+\frac{\pi r}{\varepsilon} - \ln\left(\frac{r^2}{\varepsilon^2}\right)\right) - \frac{r^2}{\Delta t^2}\right) + \mathcal{O}(g^4) \quad (66)\end{aligned}$$

[cf. Fig. 3(d)]. Trying to extract the singlet potential assuming exponential behavior of this correlator and comparing powers of g^2 as in (63) and (66), fails. There is no linear term in Δt, i.e. one obtains the physically incorrect result

$$V^1(r) = \mathcal{O}(g^4) \quad (67)$$

in contrast with the string-string correlator in temporal gauge, viz. the Wilson loop, where the parallel transport is included.

B. Gauge invariant $Q\bar{Q}Q^{\mathrm{ad}}$ correlator

As explained in Sec. IIIA2, the following gauge invariant correlation function is equivalent to $\langle W_{T^a}(r,\Delta t)\rangle$, when evaluated in temporal gauge for $a \le t_1 < t_2 < T$ [case (A)],

$$\langle W_{Q\bar{Q}Q^{\mathrm{ad}}}(r,\Delta t)\rangle = \left\langle \frac{1}{N^2-1}(N^2 W^L(r/2+s,\Delta t) \times W^R(r/2-s,\Delta t) - W_1(r,\Delta t)) \right\rangle \quad (68)$$

[cf. Fig. 3(c)]. Evaluating this correlator in Lorenz gauge one finds

$$\begin{aligned} &\lim_{\Delta t\to\infty} \langle W_{Q\bar{Q}Q^{\mathrm{ad}}}(r,\Delta t)\rangle \\ &= \frac{N^2}{N^2-1}\left(1-g^2\left(C-\frac{N^2-1}{8N\pi(r/2+s)}\right)\Delta t + \mathcal{O}(g^4)\right) \\ &\quad \times \left(1-g^2\left(C-\frac{N^2-1}{8N\pi(r/2-s)}\right)\Delta t + \mathcal{O}(g^4)\right) \\ &\quad - \frac{1}{N^2-1}\left(1-g^2\left(C-\frac{N^2-1}{8N\pi r}\right)\Delta t + \mathcal{O}(g^4)\right) \\ &= 1-g^2\left(\frac{(2N^2-1)C}{N^2-1} - \frac{1}{8N\pi}\left(\frac{N^2}{r/2+s}+\frac{N^2}{r/2-s}-\frac{1}{r}\right)\right)\Delta t \\ &\quad + \mathcal{O}(g^4) \end{aligned} \quad (69)$$

(in the $W^L W^R$-term the gluon must propagate within the same loop, i.e. either in W^L or in W^R; otherwise, the contribution vanishes, because $\mathrm{Tr}(T^a) = 0$).

As a gauge invariant observable, this loop is guaranteed to decay exponentially. Comparing powers of g^2 in (63) and (69) shows that the $Q\bar{Q}Q^{\mathrm{ad}}$ static potential is

$$V^{Q\bar{Q}Q^{\mathrm{ad}}}(r,s) = -\frac{g^2}{8N\pi}\left(\frac{N^2}{r/2+s}+\frac{N^2}{r/2-s}-\frac{1}{r}\right) + \mathrm{const} + \mathcal{O}(g^4). \quad (70)$$

For $s = 0$ (Q^{ad} is placed symmetrically between Q and $\bar{Q}$) the result simplifies to

$$V^{Q\bar{Q}Q^{\mathrm{ad}}}(r,s=0) = -\frac{(4N^2-1)g^2}{8N\pi r} + \mathrm{const} + \mathcal{O}(g^4), \quad (71)$$

i.e. is in leading nontrivial order attractive and, depending on N, by a factor $4 + 3/(N^2-1) = 4.....5$ stronger than the singlet static potential (64).

In a recent similar work a nonperturbative extraction of the color-adjoint potential from Polyakov loop correlators was suggested [30]. Similar to our treatment here and in earlier work [16], an adjoint Schwinger line appears, which however is placed at spatial infinity, or far away from the fundamental quarks. In (70) this corresponds to $s \to \infty$ (Q^{ad} is placed at spatial infinity) and one obtains

$$V^{Q\bar{Q}Q^{\mathrm{ad}}}(r,s\to\infty) = +\frac{g^2}{8N\pi r} + \mathrm{const} + \mathcal{O}(g^4), \quad (72)$$

a repulsive static potential, which is identical to the perturbative result in Lorenz gauge (65). Note, however, that perturbation theory is only valid at small quark separations, but not for large separations or even the limit $s \to \infty$, where string breaking must occur. Hence, the physical meaning of (72) is questionable. While no simulations of this observable with large s are available yet, since adjoint charges are screened we expect this correlator to decay as the ordinary Polyakov loop correlator. The physical quantity one obtains from this correlator is the singlet static potential shifted by a gluelump mass.

C. Coulomb gauge

The gluon propagator in Coulomb gauge $\partial_j A_j = 0$ is

$$\tilde{D}^{ab}_{00}(p) = \delta^{ab}\frac{1}{|\mathbf{p}|^2}, \qquad \tilde{D}_{jk}(p) = \delta^{ab}\frac{1}{p^2}\left(\delta_{jk} - \frac{p_j p_k}{|\mathbf{p}|^2}\right) \quad (73)$$

$$D^{ab}_{00}(x,y) = \frac{1}{(2\pi)^4}\int d^4p\, e^{-ip(x-y)}\tilde{D}^{ab}_{00}(p) = \delta^{ab}\frac{\delta(x_0-y_0)}{4\pi|\mathbf{x}-\mathbf{y}|}. \quad (74)$$

Starting from (59) the spatial parallel transporters can again be neglected for $\Delta t \to \infty$, while the integrals along the temporal lines give

$$\lim_{\epsilon\to 0}\int_{-\Delta t/2}^{+\Delta t/2} dt_1 \int_{-\Delta t/2}^{+\Delta t/2} dt_2 \frac{\delta(t_1-t_2)}{4\pi\epsilon} = \frac{\Delta t}{4\pi\epsilon} \quad (75)$$

$$\int_{-\Delta t/2}^{+\Delta t/2} dt_1 \int_{+\Delta t/2}^{-\Delta t/2} dt_2 \frac{\delta(t_1-t_2)}{4\pi r} = -\frac{\Delta t}{4\pi r}. \quad (76)$$

The result for $\langle W_\Sigma(r,\Delta t)\rangle$ is is the same as in Lorenz gauge. Consequently,

$$V^1(r) = -\frac{(N^2-1)g^2}{8N\pi r} + \mathrm{const} + \mathcal{O}(g^4) \quad (77)$$

is the same in both gauges, which is expected, since the Wilson loop $W_1(r,\Delta t)$ is gauge invariant. Similarly one finds the same result for the color-adjoint static potential obtained from $W_{T^a}(r, \Delta t)$ in Coulomb gauge as well as in Lorenz gauge,

$$V^{T^a}(r) = +\frac{g^2}{8N\pi r} + \text{const} + \mathcal{O}(g^4). \tag{78}$$

In Coulomb gauge a transfer matrix/Hamiltonian exists [15], the asymptotic decay in t is exponential and a comparison of powers of g^2 in (63) and W^{T^a} [which yields (78)] appears physically meaningful. However, a nonzero result without completing the gauge is in contrast to the nonperturbative evaluation, Sec. IIIB. This indicates that gauge fixing in perturbation theory is not the same as in a corresponding nonperturbative formulation. The reason might be that perturbation theory is an expansion about a free theory with classical minimum $A_\mu = 0$, which does not include averaging over all gauge equivalent gauge field configurations fulfilling the gauge condition.

V. NUMERICAL RESULTS

In this section we compute the singlet static potential $V^1(r)$ and the color-adjoint static potential in temporal gauge $V^{T^a}(r)$, which is identical to the gauge invariant static potential $V^{Q\bar{Q}Q^{\text{ad}}}$, using $SU(2)$ lattice gauge theory, where $T^a = \sigma^a/2$.

A. Lattice setup

The lattice action is the standard Wilson plaquette gauge action [Eqs. (23)–(25)]. The lattice extension is $(L/a)^3 \times T/a = 24^3 \times 48$. We have performed simulations at four different values of the coupling constant $\beta \in \{2.40, 2.50, 2.60, 2.70\}$. Observables are computed as averages over 200 essentially independent gauge link configurations.

To introduce a physical scale we have identified the Sommer parameter r_0 with 0.46 fm, which is roughly the QCD value (cf. e.g. [31,32]; the Sommer parameter is defined via the static force, $|F(r_0)r_0^2| \equiv 1.65$, $F(r) = dV^1(r)/dr$). The corresponding lattice spacings are listed in Table I.

B. The singlet and the color−adjoint/$Q\bar{Q}Q^{\text{ad}}$ static potential

We have used standard techniques, to compute the singlet and the color−adjoint/$Q\bar{Q}Q^{\text{ad}}$ static potential. We have evaluated the gauge invariant correlator diagrams shown in Fig. 2 [singlet, case (A) and adjoint, case (A)] on the 200 available gauge link configurations using translational and rotational invariance to increase statistical precision. Moreover, we have resorted to common smearing techniques:

(1) **APE smearing for spatial links** [33]
This improves the ground state overlap, i.e. increases e.g. for the matrix elements in (42) the ratio

$$\left|\frac{\langle 0_{\alpha\beta}|\hat{U}_{\alpha\beta}(\mathbf{x},\mathbf{y})|0\rangle}{\langle k'_{\alpha\beta}|\hat{U}_{\alpha\beta}(\mathbf{x},\mathbf{y})|n'\rangle}\right|, \qquad (k', n') \neq (0, 0). \tag{79}$$

This in turn allows us to extract the value of $V^1(r)$ or $V^{T^a}(r)$ from the exponential behavior of the corresponding correlator diagrams at smaller temporal separations, where also the statistical errors are smaller. We used $N_{\text{APE}} = 15$ and $\alpha_{\text{APE}} = 0.5$, where detailed equations can e.g. be found in [34], Sec. III A.

(2) **HYP2 smearing for temporal links** [35,36,37]
This amounts to using a different discretization for the action of the static color charges. It reduces the self-energy of these charges and, therefore, the extracted static potential $V^1(r)$ or $V^{T^a}(r)$ by an r-independent constant. Consequently, the exponential decay of the correlator diagram is weaker, which again results in a smaller statistical error.

Figure 4 shows V^1 and V^{T^a} in physical units. Note that at large static color charge separations both V^1 and V^{T^a} exhibit essentially the same slope. This is expected and indicates flux tube formation not only between Q and $\bar{Q}$ in

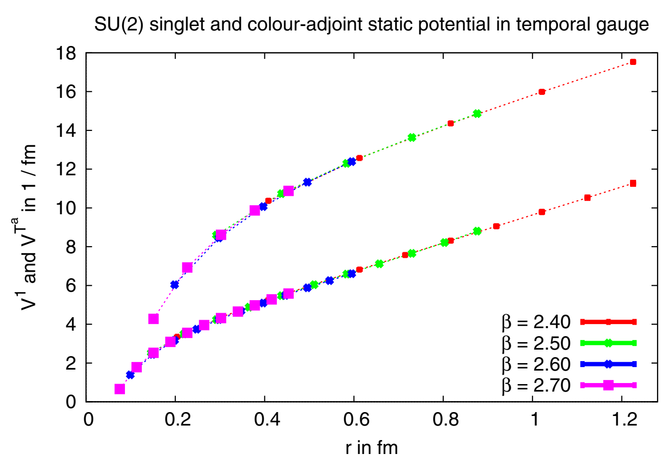

FIG. 4 (color online). V^1 (lower curve) and V^{T^a} (upper curve) as a functions of the $Q\bar{Q}$ separation r in physical units (lattice results obtained at different values of β have been shifted vertically, to compensate for the a-dependent self-energy of the static charges). For V^{T^a} the adjoint static color charge is located halfway between Q and $\bar{Q}$. Lattice results, where any of the static charges are closer than $2a$, have been omitted, because of rapidly increasing discretization errors.

TABLE I. α_s extracted from $V^1(r)$ and from $V^{T^a}(r)$.

β	a in fm	α_s^1	$\alpha_s^{T^a}$	$\Delta\alpha_s^{\text{rel}}$
2.40	0.102	0.89	0.75	17%
2.50	0.073	0.59	0.52	13%
2.60	0.050	0.43	0.40	9%
2.70	0.038	0.36	0.33	6%

the singlet case, but also between Q and $Q^{\rm ad}$ and also between $Q^{\rm ad}$ and $\bar{Q}$ in the color−adjoint/$Q\bar{Q}Q^{\rm ad}$ case.

C. Comparing lattice and perturbative results

Lattice results for the static potential are known to exhibit large discretization errors, as soon as static color charges are closer than $2a$ (for our ensembles $2a \approx 0.08$ fm…0.20 fm). On the other hand perturbative results for the static potential are only trustworthy for separations $\lesssim 0.2$ fm. Therefore, the region of overlap between lattice and perturbative results is quite small. Moreover, the leading order of perturbation theory

$$V^{1,\rm LO}(r) = -\frac{3g^2}{16\pi r} + \text{const}, \qquad V^{T^a,\rm LO}(r) = -\frac{15g^2}{16\pi r} + \text{const} \tag{80}$$

[here specialized to gauge group $SU(2)$] we have calculated in Secs. IVA and IVB is known to be a rather poor approximation (cf. e.g. [38–41]). Consequently, one can only expect qualitative agreement, when comparing the here presented lattice and perturbative results.

We perform such a comparison by determining $\alpha_s \equiv g^2/4\pi$ from the corresponding static forces $F^X(r) = dV^X(r)/dr$, $X \in \{1, T^a\}$, which we define on the lattice by finite differences. For the singlet case we use

$$\frac{V^{1,\rm lattice}(3a) - V^{1,\rm lattice}(2a)}{a} = \frac{3\alpha_s^1}{4(2.5 \times a)^2}. \tag{81}$$

This ensures that the static color charges are separated by at least $2a$, while at the same time their separation is small enough, to expect that the leading-order perturbative result is a reasonable approximation. Similarly we use

$$\frac{V^{T^a,\rm lattice}(6a) - V^{T^a,\rm lattice}(4a)}{2a} = \frac{15\alpha_s^{T^a}}{4(5 \times a)^2} \tag{82}$$

for the color-adjoint case.

The values we obtain for α_s are collected in Table I. The relative difference between α_s extracted from $V^1(r)$ and from $V^{T^a}(r)$, defined as

$$\Delta\alpha_s^{\rm rel} \equiv 2\left|\frac{\alpha_s^1 - \alpha_s^{T^a}}{\alpha_s^1 + \alpha_s^{T^a}}\right|, \tag{83}$$

is quite small, less than 10% for our two smallest lattice spacings, which is a clear sign of agreement between the lattice and the perturbative results. $\Delta\alpha_s^{\rm rel}$ is getting smaller, when the lattice spacing is decreased, which is expected, since the quality of the leading- order perturbative approximation is improving at smaller static color charge separations.

It is also interesting to note that the values for α_s increase for larger lattice spacings, i.e. for larger static color charge separations. $\alpha_s \gtrsim 1$ signals complete breakdown of perturbation theory.

VI. CONCLUSIONS

We have discussed the nonperturbative definition of a static potential for a quark antiquark pair in a color-adjoint configuration, based on Wilson loops with generator insertions in the spatial string. Leading-order perturbation theory in Lorenz gauges has long predicted the corresponding potential to be repulsive. Saturating the open adjoint indices with color-magnetic fields, as suggested in the literature [4], produces a well-defined gauge invariant observable but spectral analysis shows it to project on the color-singlet channel only. If the adjoint indices are left open, gauge fixing is required in order to obtain a nonzero result for the correlator.

Lorenz gauges violate positivity and the gauge fixed correlator no longer has purely exponential decay, thus precluding a nonperturbative definition of the potential. In temporal gauge a positive transfer matrix with well-defined charge sectors exists and the Wilson loop with generator insertions can be shown to be equivalent to a gauge invariant object, where the open charges are saturated with an adjoint Schwinger line. This correlator projects on states with the desired transformation behavior; however, the resulting potential is attractive and should be interpreted as a three-quark potential (fundamental, antifundamental and adjoint). The same qualitative behavior is found in leading-order perturbation theory once the adjoint line is included. In Coulomb gauge a positive transfer matrix exists, but the gauge is incomplete and the observable averages to zero. Imposing an additional gauge condition to render Coulomb gauge complete again introduces an adjoint static quark. The interpretation of the resulting static potential is then identical to that in temporal gauge. It thus appears impossible to reproduce the perturbatively repulsive color-adjoint potential by a nonperturbative computation based on Wilson loops, even at short distance.

ACKNOWLEDGMENTS

We thank Felix Karbstein for discussions. M. W. acknowledges support by the Emmy Noether Programme of the DFG (German Research Foundation), Grant No. WA 3000/1-1. This work was supported in part by the Helmholtz International Center for FAIR within the framework of the LOEWE program launched by the State of Hesse.

[1] W. E. Caswell and G. P. Lepage, Phys. Lett. **167B**, 437 (1986).
[2] G. T. Bodwin, E. Braaten, and G. P. Lepage, Phys. Rev. D **51**, 1125 (1995); Phys. Rev. D **55**, 5853(E) (1997).
[3] A. Pineda and J. Soto, Nucl. Phys. B, Proc. Suppl. **64**, 428 (1998).
[4] N. Brambilla, A. Pineda, J. Soto, and A. Vairo, Nucl. Phys. **B566**, 275 (2000).
[5] L. S. Brown and W. I. Weisberger, Phys. Rev. D **20**, 3239 (1979).
[6] L. D. McLerran and B. Svetitsky, Phys. Rev. D **24**, 450 (1981).
[7] S. Nadkarni, Phys. Rev. D **34**, 3904 (1986).
[8] E. V. Shuryak and I. Zahed, Phys. Rev. D **70**, 054507 (2004).
[9] N. Brambilla, J. Ghiglieri, A. Vairo, and P. Petreczky, Phys. Rev. D **78**, 014017 (2008).
[10] B. A. Kniehl, A. A. Penin, Y. Schroder, V. A. Smirnov and M. Steinhauser, Phys. Lett. B **607**, 96 (2005).
[11] A. Pineda and M. Stahlhofen, Phys. Rev. D **84**, 034016 (2011).
[12] C. Anzai, M. Prausa, A. V. Smirnov, V. A. Smirnov, and M. Steinhauser, Phys. Rev. D **88**, 054030 (2013).
[13] C. Borgs and E. Seiler, Commun. Math. Phys. **91**, 329 (1983).
[14] O. Jahn and O. Philipsen, Phys. Rev. D **70**, 074504 (2004).
[15] D. Zwanziger, Nucl. Phys. **B485**, 185 (1997).
[16] M. Wagner and O. Philipsen, in Proc. Sci., ConfinementX (**2012**) 340.
[17] G. S. Bali, Phys. Rep. **343**, 1 (2001).
[18] K. J. Juge, J. Kuti, and C. Morningstar, Phys. Rev. Lett. **90**, 161601 (2003).
[19] G. S. Bali and A. Pineda, Phys. Rev. D **69**, 094001 (2004).
[20] G. C. Rossi and M. Testa, Nucl. Phys. **B163**, 109 (1980).
[21] G. C. Rossi and M. Testa, Nucl. Phys. **B176**, 477 (1980).
[22] M. Creutz, Phys. Rev. D **15**, 1128 (1977).
[23] I. Montvay and G. Münster, *Quantum Fields on a Lattice* (Cambridge University Press, Cambridge, England, 1994).
[24] C. Gattringer and C. B. Lang, Lect. Notes Phys. **788**, 1 (2010).
[25] H. J. Rothe, World Sci. Lect. Notes Phys. **82**, 1 (2012).
[26] O. Philipsen, Nucl. Phys. **B628**, 167 (2002).
[27] M. Creutz, J. Math. Phys. (N.Y.) **19**, 2043 (1978).
[28] G. S. Bali, H. Neff, T. Düssel, T. Lippert, and K. Schilling (SESAM Collaboration), Phys. Rev. D **71**, 114513 (2005).
[29] M. Wagner (ETM Collaboration), Proc. Sci. LATTICE (**2010**) 162.
[30] G. Rossi and M. Testa, Phys. Rev. D **87**, 085014 (2013).
[31] R. Baron *et al.* (ETM Collaboration), J. High Energy Phys. 06 (**2010**) 111.
[32] M. Donnellan, F. Knechtli, B. Leder, and R. Sommer, Nucl. Phys. **B849**, 45 (2011).
[33] M. Albanese *et al.* (APE Collaboration), Phys. Lett. B **192**, 163 (1987).
[34] K. Jansen, C. Michael, A. Shindler, and M. Wagner (ETM Collaboration), J. High Energy Phys. 12 (**2008**) 058.
[35] A. Hasenfratz and F. Knechtli, Phys. Rev. D **64**, 034504 (2001).
[36] M. Della Morte, S. Dürr, J. Heitger, H. Molke, J. Rolf, A. Shindler, and R. Sommer, Phys. Lett. B **581**, 93 (2004).
[37] M. Della Morte, A. Shindler, and R. Sommer, J. High Energy Phys. 08 (**2005**) 051.
[38] A. Pineda, J. Phys. G **29**, 371 (2003).
[39] N. Brambilla, X. Garcia i Tormo, J. Soto, and A. Vairo, Phys. Rev. Lett. **105**, 212001 (2010); Phys. Rev. Lett. **108**, 269903(E) (2012).
[40] K. Jansen, F. Karbstein, A. Nagy, and M. Wagner (ETM Collaboration), J. High Energy Phys. 01 (**2012**) 025.
[41] A. Bazavov, N. Brambilla, X. Garcia i Tormo, P. Petreczky, J. Soto, and A. Vairo, Phys. Rev. D **86**, 114031 (2012).